

Solid State Spectroelectrochemistry of Redox Reactions in Polypyrrole/Oxide Molecular Heterojunctions

Andrew P. Bonifas^{†,‡} and Richard L. McCreery^{*,‡,§}

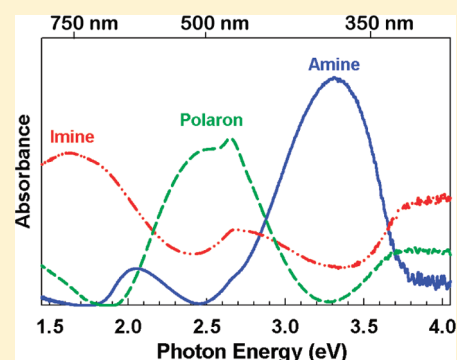
[†]Department of Materials Science and Engineering, The Ohio State University, 2041 College Road, Columbus, Ohio 43210, United States

[‡]National Institute for Nanotechnology, National Research Council Canada, Canada, T6G 2G2

[§]Department of Chemistry, University of Alberta, Canada, T6G 2R3

S Supporting Information

ABSTRACT: To understand the mechanism of bias-induced resistance switching observed in polypyrrole (PPy) based solid state junctions, in situ UV–vis absorption spectroscopy was employed to monitor oxidation states within PPy layers in solution and in PPy/metal oxide junctions. For PPy layers in acetonitrile, oxidation led primarily to cationic polaron formation, while oxidation in 0.1 M NaOH in H₂O resulted in imine formation, caused by deprotonation of polarons. On the basis of these results in solution, spectroelectrochemistry was used to monitor bias-induced formation of polarons and imines in PPy layers incorporated into solid state carbon/PPy/Al₂O₃/Pt junctions. A positive bias on the carbon electrode caused PPy oxidation, with the formation of polaron and imine species strongly dependent on the surrounding environment. The spectral changes associated with polarons or imines were stable for at least several hours after the applied bias, while a negative bias reversed the absorbance changes back to the initial PPy spectrum. These results indicate that PPy can be oxidized in nominally solid state devices, and the formation of stable polarons is dependent on the tendency for deprotonation of the polaron to the imine. Since PPy conductivity depends strongly on the polaron concentration, monitoring its concentration is critical to determining resistance switching mechanisms. Furthermore, the importance of ion mobility and OH[−] generation through H₂O reduction at the Pt contact are discussed.



Conjugated polymers are a versatile class of organic materials with structure dependent electronic properties applicable to a wide range of technological applications.¹ One such system is polypyrrole (PPy), a conjugated polymer that has been employed in a variety of applications including nonvolatile memory, sensors, corrosion protection, actuators, and fuel cells.^{2–5} The chemical structure of PPy offers a rich electrochemical platform suitable for both polaron doping and proton exchange (acid/base) reactions on the nitrogen sites on each pyrrole unit. Generation of polarons from the neutral PPy structure results in increased conductivity, and deprotonation of polarons produces imine species with decreased conductivity due to the lack of resonance stabilization of the polaron.^{3,6,7} The conductivity of PPy depends strongly on doping and hybridization, with a conductivity increase of many orders of magnitude typically observed upon polaron formation by a one-electron oxidation

A wide variety of nonvolatile memory devices based on “resistance switching” have been proposed, in which a material has two metastable states with different conductivity. Often referred to as “resistance random access memory” (RRAM), these solid state memory devices may be based on inorganic⁸ or organic materials⁹ and often involve redox reactions. As stated in the comprehensive reviews cited above, the switching mechanism for a majority of the reported resistance switching

devices is not well understood, in part because characterization of the thin and often “buried” active layer is difficult and complicates the determination of the resistance switching mechanism. We have previously reported RRAM devices based on “dynamic doping”, in which the bias induced conductance changes are attributed to the electrochemical modulation between Ti oxidation states in the case of TiO₂^{10,11} or the polaron concentration in polypyrrole layers.² In the case of PPy/TiO₂ devices, we proposed that both layers are cooperatively “doped” during the same bias pulse, which may be reversed by an opposite polarity bias pulse for at least 10³ cycles.² For memory devices based on conducting polymers, the reported memory phenomenon has been shown to be sensitive to the experimental conditions and the presence of ions.¹²

A significant challenge in determining the mechanism of memory devices is the difficulty of monitoring structure and dynamics of very thin (<50 nm) molecular layers covered by opaque metallic “contacts”.¹³ Optical absorbance spectroscopy is an attractive method to probe chemical states within PPy layers since the UV–vis–NIR absorbance strongly depends on

Received: December 9, 2011

Accepted: January 30, 2012

Published: January 30, 2012

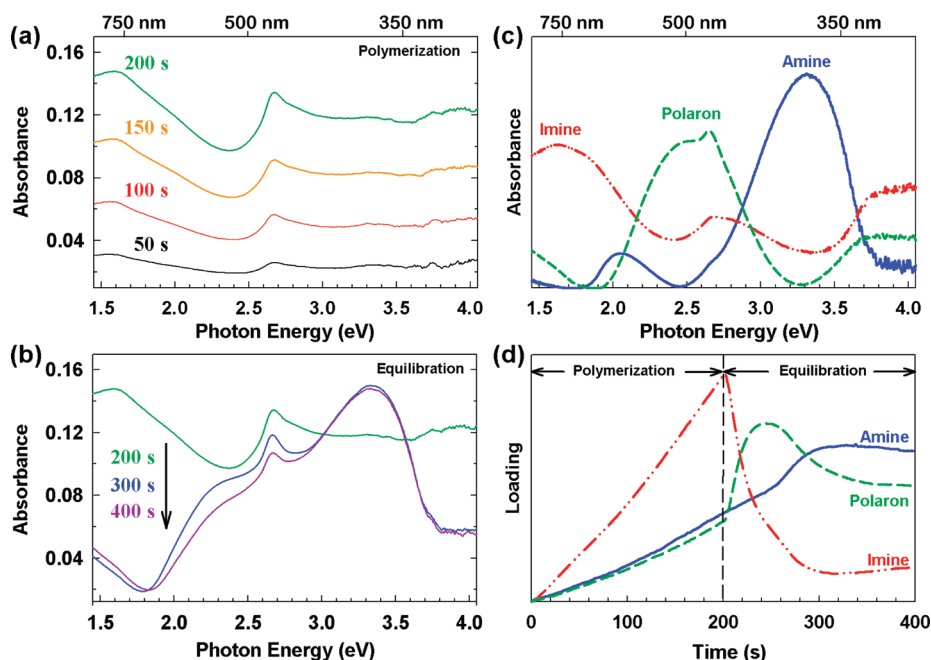


Figure 1. In situ absorbance during polymerization and equilibration of PPy. (a) Absorbance spectra during electrochemical polymerization of a PPy layer on a Pt/carbon contact. (b) Absorbance spectra during equilibration of the formed PPy layer after polymerization. (c) MCR calculated spectra of three components in the PPy layer. Spectra assigned with XPS, theoretical calculations, and spectroelectrochemistry analysis. (d) MCR calculated loading of the three components during polymerization and equilibration.

the oxidation state, conjugation, and chemical bonding within PPy^{14–16} and can nondestructively probe structural changes within functioning devices. The well established field of spectroelectrochemistry has been used previously on PPy layers in an electrolyte solution, allowing complementary structural and electrochemical analysis.^{14,17,18} Applying the fundamentals of spectroelectrochemistry to solid state devices, we previously showed that in situ optical absorbance spectroscopy can monitor the chemical structure of a 2–5 nm thick molecular layer incorporated in a solid state junction.¹⁹

In this contribution, we demonstrate in situ optical absorbance to characterize the chemical structure of PPy layers in active electronic devices. We used these absorbance spectra to investigate the chemical changes within PPy layers operating in nominal solid state devices consisting of PPy/oxide junctions. Absorbance changes of the PPy/oxide junctions under an applied bias were correlated with changes in the PPy chemical structure, and these changes are quite dependent on junction composition and environment.

EXPERIMENTAL SECTION

Schematics of the spectroelectrochemical configuration are shown in Supporting Information for solution (Figure S1) and solid state (Figure S2) experiments and are similar to that reported previously.¹⁹ A detailed experimental procedure is included in Supporting Information for both the solid state and solution experiments. Briefly, optically transparent carbon substrate electrodes (OTE) were formed by successive e-beam evaporation of Cr, Pt, and carbon on fused silica plates. Polypyrrole was formed on the Pt/C surface through electrochemical oxidation in 0.1 M solution of pyrrole (Py) in acetonitrile (MeCN) containing 0.1 M tetrabutylammonium tetrafluoroborate (TBABF₄). A constant applied oxidation current of 0.1 mA·cm⁻² for 200 s resulted in ~20 nm thick PPy layers, as determined by a scratching technique with AFM and

confirmed with spectroscopic ellipsometry.^{2,20} The observed PPy thickness implies a current efficiency for polymerization of ~25%. The PPy layer was allowed to equilibrate at open circuit for >100 s or, in some cases, reduced at -1 V vs Ag/Ag⁺ for 100 s, as described for individual experiments below. The top oxide/metal contacts were deposited on the PPy layers with e-beam evaporation through a shadow mask, resulting in a cross-bar junction with an active area of 4 × 4 mm.

RESULTS

The results are discussed first for the polymerization and electrochemistry of the PPy layers in electrolyte solutions, followed by in situ absorbance of PPy layers incorporated in solid state PPy/oxide junctions. Absorbance spectra were acquired during the electrochemical polymerization of pyrrole in TBABF₄/MeCN electrolyte to form a PPy layer on the transparent Pt/carbon contact, and are shown in Figure 1a. The approximate linearity of absorbance with deposition time implies a constant polymerization rate, and the consistency of the spectra implies that the relative concentrations of PPy species do not significantly change as the thickness of the PPy increases. After electrochemical polymerization ($t > 200$ s), the PPy layer was disconnected from the potentiostat and absorbance spectra were recorded, as shown in Figure 1b. Large absorbance changes were observed within 100 s after polymerization, and the presence of an absorbance increase between 3.0 and 3.6 eV verifies that the absorbance changes cannot be due simply to the loss of PPy at the Pt/carbon surface. Considering polymerization occurred at about 500 mV vs Ag/Ag⁺, electronic and structural reorganization would be expected as the PPy layer equilibrates within the pyrrole solution. The BF₄⁻ counterion is expected to be at least partially mobile during the observed equilibration, permitting charge compensation among the various PPy species.

Multivariate curve resolution (MCR) analysis using “PLS tool box” from eigenvector Research was performed on the spectra in Figure 1a,b to determine the principal absorbing species and their relative concentrations. For the MCR analysis, 200 spectra obtained during polymerization and 200 spectra obtained during equilibration at open circuit comprised the input data set. No preprocessing was performed, and the only constraints on the analysis were non-negativity of both spectra and contributions. The three principle components shown in Figure 1c accounted for 98% of the variation in the raw spectra. Including a fourth component accounted for 99.5% of the variance, but the fourth component had a spectrum similar to that of the polaron and no significant additional components were indicated. The spectrum loadings (relative species fractions) during polymerization and equilibration are shown in Figure 1d, indicating simultaneous formation of three components during electrochemical polymerization, followed by significant changes in relative concentrations during equilibration at OCP. The identification of two of the spectral components as the neutral amine (~ 3.3 eV) and polaron (~ 2.5 eV) in Figure 1c are based on previous experimental reports.^{7,18} The lower energy band has been attributed to a bipolaron^{16,18,21} but has been reported to absorb at energies below 1.4 eV (>900 nm) rather than the 1.7 eV (730 nm) observed in Figure 1c. Lee and Swager have reported more recently that the polaron is subject to deprotonation to an imine, particularly at $\text{pH} > 3$. Spectroelectrochemical results at elevated pH combined with X-ray photoelectron spectroscopy (XPS) and theoretical results described below lead to the assignment of the 1.7 eV absorption as the imine resulting from deprotonation of the polaron. While some bipolaron formation during polymerization cannot be ruled out, it appears to be a minor component.

The assignment of the ~ 1.7 eV absorption is assisted by the spectroelectrochemistry of the PPy film in electrolyte not containing pyrrole, shown in Figure 2. Figure 2a shows the change in absorbance relative to the initial spectrum (ΔA) of PPy layers in TBABF₄/MeCN with pyrrole monomer absent, with the potential held at the indicated values. For positive potentials relative to the OCP, an increase in absorbance at 2.2–2.6 eV and a decrease in absorbance at 3.2–3.5 eV were observed. As reported by several groups, oxidation in MeCN results in the formation of polaron species, which is consistent with our assignments in Figure 1c as the generation of polarons should increase the absorbance between 2.2 and 2.6 eV^{3,16} and decrease that due to the neutral amine (3.2–3.5 eV). During an applied reducing potential, the absorbance decrease between 2.2 and 2.6 eV and increase between 3.2 and 3.5 eV are consistent with the reduction of the polarons to neutral amines. Figure 2b shows the same experiment in 0.1 M NaOH in water, for the same potential range. The neutral amine absorbance at 3.2–3.5 eV is still modulated by potential, but the lower energy band is now near 1.7 eV (~ 730 nm).

The absorbance changes in basic solution indicate that the PPy is oxidized to the imine and that the process is chemically reversible. As proposed previously,^{3,7,22} oxidation of the neutral amine to the polaron may be followed by deprotonation to the imine, as shown schematically in Figure 3. The spectroelectrochemistry of PPy films in nonaqueous and basic electrolyte shown in Figure 2 is entirely consistent with the MCR results during film formation, and the absorbance peak positions permit direct monitoring of changes in the relative contributions of each component. The assignment of the 1.7 eV band as

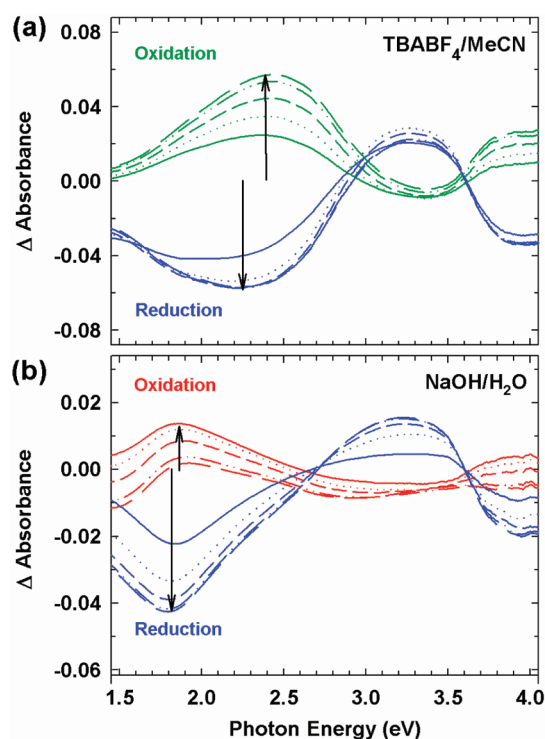


Figure 2. Spectroelectrochemistry of PPy layers between ± 500 mV vs the open circuit potential in 100 mV intervals. (a) Absorbance spectra in MeCN containing 0.1 M TBABF₄. (b) Absorbance spectra in H₂O containing 0.1 M NaOH. Spectra are referenced to the initial PPy layer on a Pt/carbon contact in the respective electrolyte solution.

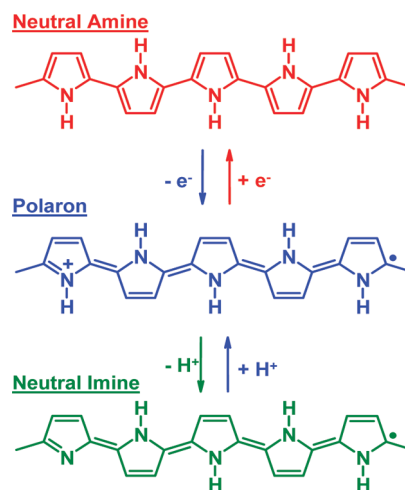


Figure 3. Redox and deprotonation reactions of the PPy films, with imine formation favored in basic solution. Note that only one resonance form for each species is shown and that the electrons in both the polaron and imine are delocalized over several pyrrole rings.³

the imine resulting from deprotonation of the polaron is also consistent with the XPS and theoretical calculations described below.

Figure S5 in Supporting Information shows the N(1s) XPS peak of an electrochemically polymerized PPy layer on Pt/carbon contacts before and after electrochemical reduction. Analysis of the XPS N(1s) peak has been widely used to determine the nitrogen oxidation state of PPy.^{23,24} For the as-deposited and reduced PPy layers, the N(1s) peaks were deconvoluted into three components centered at 397.8, 399.8,

and 402.1 eV. The peak at 399.8 eV has been identified as the neutral amine-like nitrogen, the peak at 402.1 eV as the positively charged polaron, and the peak at 397.8 eV as the neutral imine-like nitrogen.^{7,25} The 397.8 eV peak has been reported for "overoxidized" PPy and was assigned to imine sites.^{7,23} Both the imine and polaron bands decrease relative to the amine upon electrochemical reduction of the PPy film. It should be noted that since the XPS spectra were obtained after an air transfer of the sample from the electrolyte solution to the UHV chamber, the film might have partially reoxidized after electrochemical reduction. The concentration of BF_4^- incorporated in the PPy layers was determined by the F(1s) XPS spectra, shown as insets in Figure S5 in Supporting Information. For the as-grown PPy layer, the F/N ratio was 0.8, indicating partial oxidation of the PPy in the film, consistent with Figure 1d. After electrochemical reduction, the lack of an observable F(1s) band shows that BF_4^- is expelled from the PPy layer and the polaron and neutral amine levels are at least partially reduced.

Time dependent density functional theory (TDDFT) was used to optimize the structure and calculate the optical transitions of the neutral amine, neutral imine, and positively charged polaron on a pyrrole pentamer, with the results listed in Table 1. TDDFT was performed with Gaussian '03 using

Table 1. TDDFT Calculated Excitation Energies and Their Oscillator Strength^a

pentamer (charge)	calculated excitation energies ^b eV (oscillator strength)
all amines (0)	3.9 (0.01); 3.6 (0.00); 3.3 (0.01); 2.8 (1.20)
all amines (+1)	3.6 (0.10); 3.1 (0.07); 2.4 (0.53); 2.3 (0.08)
single imine (0)	3.0 (0.40); 2.7 (0.97); 1.9 (0.04); 1.8 (0.02)

^aExcitation (absorption) energies for a pentamer containing all amines, a single polaron, or a single imine. ^bTop four excitations based on oscillator strength.

B3LYP/6-31+G(d,p), with diffuse functions added to the basis set to correctly describe the Rydberg state.²⁶ Modeling PPy with a pentamer allowed an estimation of the expected absorbance trends, where the pentamer was at the limit of our computing capacity. For the imine pentamer, a hydrogen atom was removed from the center nitrogen site on the pentamer. The neutral amine pentamer had the highest excitation energies, and the polaron and imine excitations occurred at lower energies. Note that all of the predicted absorptions decrease in energy in the order amine > polaron > imine, as observed experimentally. This red-shift in excitation energy is likely due to the transition from the neutral amine to a more conjugated, planar geometry in the polaron and imine, allowing increased electron delocalization. As additional confirmation, experimentally measured absorbance spectra of polyaniline show the same trend for similar amine, polaron, and imine structures.^{5,27}

The solution spectroelectrochemistry, XPS, pH dependence, and TDDFT are all consistent with the oxidation mechanism shown in Figure 3, with an additional possibility of bipolaron formation coincident with imine formation. We now consider the case of an electrochemically formed PPy layer in a partially transparent solid state carbon/PPy/oxide/Pt molecular heterojunction. PPy/oxide junctions were fabricated from electrochemically reduced PPy layers by evaporation of $\text{Al}_2\text{O}_3/\text{Pt}$ or TiO_2/Pt as the top contacts (details in Supporting Information). Figure 4a shows bias induced absorbance changes

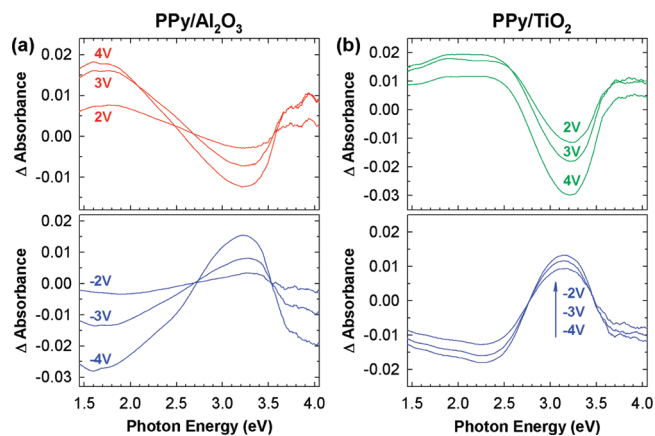


Figure 4. In situ absorbance spectra of PPy junctions during an applied bias at ambient lab conditions. PPy was reduced electrochemically before deposition of oxide and Pt layers. Absorbance changes are referenced to the initial absorbance of the PPy/oxide junctions. Indicated bias voltages were applied for 100 ms each to the initial device in the order: +2, +3, +4, -2, -3, and -4 V. (a) Absorbance changes for PPy/ Al_2O_3 . (b) Absorbance changes for PPy/ TiO_2 .

of solid state PPy/ Al_2O_3 and PPy/ TiO_2 junctions in ambient laboratory conditions, with no intentional electrolyte or reference electrode. For the PPy/ Al_2O_3 junctions, a positive bias caused an increase in absorbance between 1.7 and 1.9 eV and a decrease in absorbance between 2.8 and 3.5 eV, consistent with the formation of neutral imines from neutral amines. With a negative bias, the absorbance changes were consistent with formation of neutral amines, showing the amine/imine distribution can be modulated in the solid state by switching the polarity of the applied bias. The negative ΔA occurring after negative voltage bias indicates that the PPy film was not completely reduced in the initial junction, consistent with the XPS results of Figure S5, Supporting Information. The bias-induced absorbance changes were repeatable for at least tens of voltage cycles. For all PPy/oxide junctions studied, the reported absorbance changes were stable after the applied bias was removed for at least 2 h.

Bias induced absorbance changes of PPy/ TiO_2 junctions in ambient conditions are shown in Figure 4b. The shape of the ΔA spectra are different for the PPy/ TiO_2 compared to PPy/ Al_2O_3 junctions, with a larger change observed in the 2.5 eV region corresponding to the polaron. With a positive bias, a broad absorbance increase between 1.7 and 2.6 eV and an absorbance decrease between 3.0 and 3.4 eV were observed, consistent with the formation of both polarons and imines from the neutral amine. As was the case for PPy/ Al_2O_3 , the absorbance changes can be cycled for at least tens of cycles. When the PPy layer was replaced with a redox-inactive C_{10}N molecular monolayer, absorbance changes were below the detection limit for the same bias range. It should be noted that while the absorbance changes in both panels of Figure 4 are consistent with redistribution between amine, polaron, and imine species, optical transitions in polypyrrole are subject to solvent and counterion effects.²⁸ Such effects may be pronounced in the nominally solid state junctions reported here.

Figure 5 shows the effect of the environment on the observed bias induced absorbance changes. When the spectrometer chamber was purged with dry N_2 in the presence

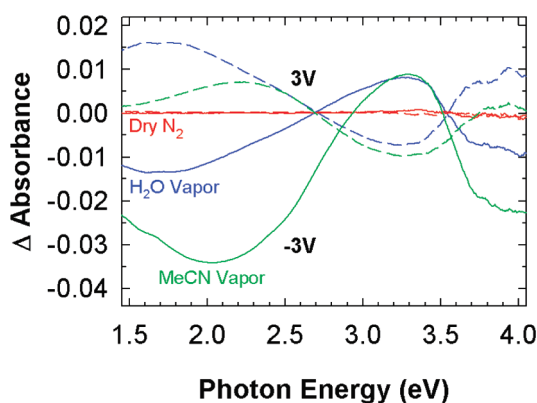


Figure 5. Biased induced absorbance changes of PPy/Al₂O₃ junctions in various environments. Absorbance changes in dry N₂ (red), dry N₂ bubbled through H₂O (blue), and dry N₂ bubbled through MeCN (green) under an applied voltage of ± 3 V.

of anhydrous calcium sulfate as a desiccant, absorbance changes in response to an applied bias were absent for all junction types examined. Exposure of the dried junctions to ambient lab conditions for 1 h restored the bias-induced absorbance changes to responses similar to those shown in Figure 4. Absorbance changes for PPy/Al₂O₃ junctions with an applied bias of ± 3 V are shown in Figure 5 for a dry environment and after exposure to dry N₂ saturated with H₂O or MeCN. For the PPy/Al₂O₃ junctions, bias-induced absorbance changes in the presence of H₂O vapor are similar to absorbance changes at ambient conditions and consistent with modulation between the neutral imine and amine. In the presence of MeCN, the bias induced absorbance changes indicate modulation between the polaron and amine species. These results are analogous to those of Jernigan et al., who reported that exposure to a gas phase solvent can be used to induce redox events in a poly(Os-(bpy)₂(vpy)₂)(ClO₄)₂ layer sandwiched between two metallic contacts.²⁹

In order to probe the role of deprotonation in the PPy oxidation mechanism, *p*-nitrophenol was deposited between the PPy and Al₂O₃ layer, and the bias was applied in the ambient environment. The absorbance changes under bias are shown in Figure 6. In solution, NP is a weak acid with a reported pK_a of

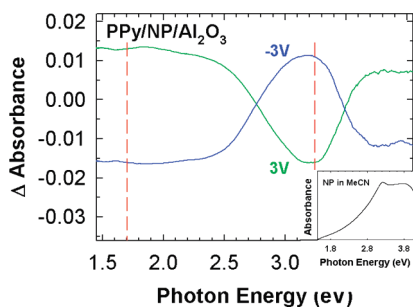


Figure 6. Bias induced absorbance changes of a PPy/NP/Al₂O₃ junction in ambient lab conditions. Dashed lines represent the maximum absorbance changes observed in PPy/Al₂O₃ junctions under the same experimental conditions (Figure 5a). Inset is the solution spectrum of NP in MeCN.

7.16 in H₂O and 8.45 in a MeCN/H₂O mixture.³⁰ The absorbance changes are similar to those for the PPy/TiO₂ junctions, where the concentration of both the polarons and imines are modulated with the applied bias. In comparison to

the PPy/Al₂O₃ junction, incorporation of the NP layer results in larger bias induced modulation of the polaron concentration and less imine formation.

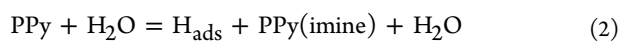
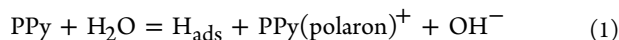
DISCUSSION

Combining the UV–vis spectroelectrochemistry and pH dependence with XPS analysis (Figure S5, Supporting Information) and the MCR analysis (Figure 1), relative concentrations of the neutral amine, neutral imine, and positively charged polaron were monitored during electrochemical polymerization and redox processes of a ~ 20 nm thick PPy film in electrolyte solution. The XPS and MCR results indicate that the amine is the dominant species in the as-formed film and that the amine is the strongest absorber at ~ 3.4 eV. An estimate of the concentration modulation induced by potential excursions is available from comparison of Figure 1b with Figure 2. The absorbance at 3.4 eV is mostly due to the amine, and its value after equilibration (0.15 absorbance units) corresponds to a film which is $>80\%$ amine, based on the XPS. Therefore, the 0.03 unit absorbance modulation evident in Figure 2 corresponds to a concentration change of $\sim 16\%$ of the total neutral amine present. Since the change in conductivity from the undoped (amine) to doped (polaron) states of polypyrrole is greater than a factor of 10^8 , a $\sim 16\%$ concentration change implies a large change in conductivity, depending on the initial doping level.⁶

The conductivity change associated with conversion from polaron to imine depends on the transport dimensionality and the concentration of polarons. Deprotonation of polaron causes a significant decrease in conductivity for one-dimensional conduction paths but a much smaller decrease for conduction paths of higher dimensionalities.³¹ All spectra obtained in electrolyte returned to their initial absorbance spectrum when the applied potential was removed, indicating that the electrochemically formed polaron and imine are not stable at OCP. As shown in Figure 2, modulation between the amine as the reduced form and polaron or imine in the oxidized state strongly depended on the surrounding environment and its effect on polaron deprotonation.

The spectroelectrochemical results of molecular heterojunctions (Figures 4 and 5) demonstrate that bias-induced redox events can occur in nominally solid state devices, but the magnitude of structural changes is strongly dependent on conditions and junction components. The ~ 0.02 ΔA observed in the solid state at 3.4 eV corresponds to a $\sim 11\%$ change in the neutral amine concentration, still sufficient for a significant change in conductivity. For in situ spectra of PPy/oxide junctions acquired in a dry N₂ environment, bias-induced absorbance changes were below the detection limit for all junctions tested. The lack of an observable absorbance change indicates charge transfer between the Pt/carbon contact and PPy layer does not occur in a dry N₂ environment. Since the absorbance spectra are sensitive only to concentration changes, bias-induced spatial redistribution of charged polaron species is not expected to result in an absorbance change. The fact that ambient air or H₂O saturated N₂ restored the absorbance changes of dry devices indicate that H₂O plays a key role in polaron formation, even in nominally solid state PPy/oxide devices. Having water present in the junction likely solvates ions, greatly increasing their mobility, and permits charge compensation for the cationic polarons. Without mobile ions, a space charge would develop in the PPy layer, which would rapidly suppress further oxidation. Water may stabilize the

polaron by decreasing the reorganization energy associated with the oxidation of the neutral amine to the polaron species and screening the positive charge. In addition, reduction of water to OH^- and chemisorbed hydrogen at the Pt contact may provide the redox counter reaction needed to form stable polarons. Under bias, mobile OH^- ions could migrate to the PPy layer to either stabilize the polaron or cause imine formation through polaron deprotonation. The resulting cell reaction is one of the following:



H_2O is included on both sides of reaction 2 to emphasize that electrochemical reduction of H_2O generates OH^- ions at the Pt contact that can migrate to the PPy layer and deprotonate the polaron to reform H_2O . A schematic of this mechanism is shown in Figure 7. Note that H_2O can serve three roles in the

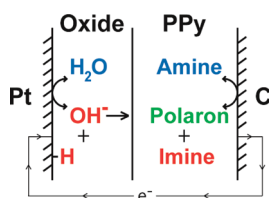


Figure 7. Proposed mechanism for the observed bias induced absorbance changes in PPy/oxide junctions in the presence of water vapor. Positive bias creates mobile OH^- ions that can either stabilize the polaron or deprotonate the polaron to form the imine. For all junctions measured, a negative bias causes the neutral amine species to reform.

process: a counter reaction for PPy oxidation, a solvent to increase ion mobility, and a base to accept protons during imine formation. As shown in Figure 6, the addition of *p*-nitrophenol to the device significantly increases polaron absorption and concentration, since NP can react with OH^- and reduce polaron deprotonation to the imine.

The observed bias induced absorbance changes resulting from the formation of polarons and imines were stable for at least 2 h after the applied bias for all PPy/oxide junctions investigated, and the stability of the polaron species is critical to retention in possible resistance switching memory applications. The open circuit voltage across the junction after the applied bias decreased to zero in less than 60 s after removal of the bias. In order to observe stable absorbance changes and a negligible open circuit voltage, ion migration must have occurred, allowing charge compensation and/or deprotonation of the polaron. Regarding the stability of the electrochemically formed polarons and imines, the observed stability can be explained by low counterion mobility in the absence of an applied bias, low proton mobility caused by chemisorbed H on the Pt contact, or large reorganization energy associated with redox events.

While PPy/ Al_2O_3 junctions exhibited modulation between neutral amine and neutral imine species in the presence of H_2O vapor, bias induced absorbance changes of PPy/ Al_2O_3 junctions in MeCN saturated N_2 indicate a higher concentration of polarons compared to imines. In contrast to H_2O , MeCN is an aprotic solvent expected to retard deprotonation of a PPy polaron and suppress imine formation. While MeCN should increase ion mobility, it cannot be reduced at the Pt surface to generate OH^- counterions. Although the counter reaction for

the PPy/ Al_2O_3 junctions in MeCN vapor is not obvious, the increased absorbance changes associated with the polaron indicates that OH^- migration into the PPy layer is unlikely. Possible stabilizing species include bias-induced point defects in the Al_2O_3 layer or unintentional counterions in the evaporated Al_2O_3 layer. Trace water is still expected to be chemisorbed in the Al_2O_3 layer in our dry N_2 atmosphere and may undergo electrochemical reduction on the Pt contact.³² For a 5% change in the polaron fraction, about 10^{-9} mol/cm² of negative counterions are needed for charge balance. It is possible adsorbed H_2O in the Al_2O_3 layer is sufficient to allow charge balance, but the mechanism must involve an ion that does not deprotonate the polaron.

For PPy/ TiO_2 junctions, the biased induced absorbance changes are consistent with the generation of both polarons and imines in the presence of H_2O . Under an applied bias, TiO_2 layers have been shown to form intermediate oxidation states^{10,11} and negative point defects such as oxygen vacancies and Ti interstitials,^{11,33} which could provide charge balance for formed polarons. The absorbance changes apparent in Figure 4b for PPy/ TiO_2 devices are unlikely caused by the TiO_2 alone, since similar changes were observed in PPy/ Al_2O_3 devices and bias induced absorbance changes were absent for octylamine/ TiO_2 junctions. Also, the additional polaron formation with TiO_2 compared to Al_2O_3 may result from differences in the acid–base properties of the two oxides in the presence of H_2O .

CONCLUSIONS

We have used XPS, MCR analysis of the absorption spectra during electrochemical PPy polymerization on Pt/carbon electrodes, and solution based electrochemistry of PPy layers to determine the individual absorbance spectra of the neutral amine, polaron, and neutral imine species in PPy films. We showed that bias induced formation of PPy polarons and imines in solid state devices is strongly influenced by the surrounding environment and oxide composition, mediated by the tendency for polaron deprotonation. Since commonly applied voltages for organic thin film electronic devices often exceed several volts, electrochemical redox events in the conjugated polymer layer are expected to occur, especially in the presence of residual water and the commonly applied bias range of 10–50 V.³⁴ The ability to probe “buried” organic layers in active devices allows these potential redox events to be monitored, thus providing complementary structural information for the observed electronic changes. We are currently correlating bias-induced changes in UV–vis and Raman spectra³⁵ with conductivity changes for PPy and polythiophene devices, allowing insight into the mechanism behind observed resistance changes.

ASSOCIATED CONTENT

Supporting Information

Six supporting figures and one table referred to in the main text, showing cell schematics, current and potential traces during PPy deposition, XPS spectra, and additional absorbance results. This material is available free of charge via the Internet at <http://pubs.acs.org>.

AUTHOR INFORMATION

Corresponding Author

*Tel.: 780-641-1760. E-mail: richard.mccreery@ualberta.ca.

Notes

The authors declare no competing financial interest.

ACKNOWLEDGMENTS

Authors would like to acknowledge Dimitre Karpuzov and the Alberta Centre for Surface Engineering and Science for collecting the XPS spectra and Dr. Gino DiLabio, Dr. Vincent Wright, and Dr. David Rider for their scientific discussions. This work was supported by the National Science Foundation, The National Research Council Canada, and Alberta Ingenuity Technology Futures.

REFERENCES

- (1) Sugiyasu, K.; Swager, T. M. *Bull. Chem. Soc. Jpn.* **2007**, *80*, 2074–2083. Lee, K.; Cho, S.; Park, S. H.; Heeger, A. J.; Lee, C. W.; Lee, S. H. *Nature* **2006**, *441*, 65–68.
- (2) Barman, S.; Deng, F. J.; McCreery, R. L. *J. Am. Chem. Soc.* **2008**, *130*, 11073–11081.
- (3) Lee, D.; Swager, T. M. *Chem. Mater.* **2005**, *17*, 4622–4629.
- (4) Janata, J.; Josowicz, M. *Nat. Mater.* **2003**, *2*, 19–24. Zhao, J. H.; Thomson, D. J.; Pilapil, M.; Pillai, R. G.; Rahman, G. M. A.; Freund, M. S. *Nanotechnology* **2010**, *21*, 134003. Lu, W.; Fadeev, A. G.; Qi, B. H.; Smela, E.; Mattes, B. R.; Ding, J.; Spinks, G. M.; Mazurkiewicz, J.; Zhou, D. Z.; Wallace, G. G.; MacFarlane, D. R.; Forsyth, S. A.; Forsyth, M. *Science* **2002**, *297*, 983–987. Berdichevsky, Y.; Lo, Y. H. *Adv. Mater.* **2006**, *18*, 122–125. Xu, L.; Wang, J. X.; Song, Y. L.; Jiang, L. *Chem. Mater.* **2008**, *20*, 3554–3556. Rizzi, M.; Trueba, M.; Trasatti, S. P. *Synth. Met.* **2010**, *161*, 23–31. Zhitomirsky, I. *Surf. Eng.* **2010**, *27*, 1–4.
- (5) Ramanavicius, A.; Ramanaviciene, A.; Malinauskas, A. *Electrochim. Acta* **2006**, *51*, 6025–6037.
- (6) Saunders, B. R.; Fleming, R. J.; Murray, K. S. *Chem. Mater.* **1995**, *7*, 1082–1094.
- (7) Neoh, K. G.; Lau, K. K. S.; Wong, V. V. T.; Kang, E. T.; Tan, K. L. *Chem. Mater.* **1996**, *8*, 167–172.
- (8) Waser, R.; Dittmann, R.; Staikov, G.; Szot, K. *Adv. Mater.* **2009**, *21*, 2632–2663.
- (9) Scott, J. C.; Bozano, L. D. *Adv. Mater.* **2007**, *19*, 1452–1463. Heremans, P.; Gelinck, G. H.; Muller, R.; Baeg, K.-J.; Kim, D.-Y.; Noh, Y.-Y. *Chem. Mater.* **2010**, *23*, 341–358.
- (10) Nowak, A. M.; McCreery, R. L. *Anal. Chem.* **2004**, *76*, 1089. Wu, J.; McCreery, R. L. *J. Electrochem. Soc.* **2009**, *156*, P29–P37.
- (11) Wu, J.; Mobley, K.; McCreery, R. J. *Chem. Phys.* **2007**, *126*, 24704.
- (12) Mandell, A.; VanBuskirk, M. A.; Spitzer, S.; Krieger, J. H. Polymer memory device with variable period of retention time. U.S. Patent # 7,199,394, 2007. Krieger, J. H.; Trubin, S. V.; Vaschenko, S. B.; Yudanov, N. F. *Synth. Met.* **2001**, *122*, 199. Krieger, J. H.; Spitzer, S. Switchable memory diode—a new memory device. U.S. Patent # 7,157,732, 2007.
- (13) Bergren, A. J.; McCreery, R. L. *Annu. Rev. Anal. Chem.* **2011**, *4*, 173–195. McCreery, R. L. *Anal. Chem.* **2006**, *78*, 3490–3497.
- (14) Skaarup, S.; West, K.; Zachaustriansen, B.; Jacobsen, T. *Synth. Met.* **1992**, *51*, 267–275.
- (15) Christensen, P. A.; Hamnett, A. *Electrochim. Acta* **1991**, *36*, 1263–1286. Okur, S.; Salzner, U. J. *Phys. Chem. A* **2008**, *112*, 11842–11853. Turcu, R.; Brie, M.; Leising, G.; Niko, A. *Synth. Met.* **1999**, *100*, 217–221.
- (16) Bredas, J. L.; Scott, J. C.; Yakushi, K.; Street, G. B. *Phys. Rev. B* **1984**, *30*, 1023–1025.
- (17) Genies, E. M.; Pernaut, J. M. *J. Electroanal. Chem.* **1985**, *191*, 111–126. Kim, Y. T.; Collins, R. W.; Vedam, K.; Allara, D. L. *J. Electrochem. Soc.* **1991**, *138*, 3266–3275.
- (18) Amemiya, T.; Hashimoto, K.; Fujishima, A.; Itoh, K. *J. Electrochem. Soc.* **1991**, *138*, 2845–2850.
- (19) Bonifas, A. P.; McCreery, R. L. *Chem. Mater.* **2008**, *20*, 3849–3856.
- (20) Anariba, F.; DuVall, S. H.; McCreery, R. L. *Anal. Chem.* **2003**, *75*, 3837–3844.
- (21) Cabala, R.; Skarda, J.; Potje-Kamloth, K. *Phys. Chem. Chem. Phys.* **2000**, *2*, 3283–3291. Kaufman, J. H.; Colaneri, N.; Scott, J. C.; Street, G. B. *Phys. Rev. Lett.* **1984**, *53*, 1005–1008.
- (22) Lee, D.; Swager, T. M. *J. Am. Chem. Soc.* **2003**, *125*, 6870–6871. Li, Y. F.; Qian, R. Y. *Synth. Met.* **1988**, *26*, 139–151.
- (23) Jaramillo, A.; Spurlock, L. D.; Young, V.; Brajter-Toth, A. *Analyst* **1999**, *124*, 1215–1221.
- (24) Kim, D. Y.; Lee, J. Y.; Kim, C. Y.; Kang, E. T.; Tan, K. L. *Synth. Met.* **1995**, *72*, 243–248.
- (25) Kim, D. Y.; Lee, J. Y.; Kim, C. Y.; Kang, E. T.; Tan, K. L. *Synth. Met.* **1995**, *72*, 243–248. Skotheim, T. A.; Florit, M. I.; Melo, A.; O’Grady, W. E. *Phys. Rev. B* **1984**, *30*, 4846. Kang, E. T.; Neoh, K. G.; Tan, K. L. *Adv. Polym. Sci.* **1993**, *106*, 135–190.
- (26) DiLabio, G. A.; Litwinienko, G.; Lin, S. Q.; Pratt, D. A.; Ingold, K. U. *J. Phys. Chem. A* **2002**, *106*, 11719–11725. Kwasniewski, S. P.; Deleuze, M. S.; Francois, J. P. *Int. J. Quantum Chem.* **2000**, *80*, 672–680.
- (27) Nekrasov, A. A.; Ivanov, V. F.; Vannikov, A. V. *J. Electroanal. Chem.* **2000**, *482*, 11–17.
- (28) Lacroix, J. C.; Chane-Ching, K. I.; Maquere, F.; Maurel, F. *J. Am. Chem. Soc.* **2006**, *128*, 7264–7276.
- (29) Jernigan, J. C.; Chidsey, C. E. D.; Murray, R. W. *J. Am. Chem. Soc.* **1985**, *107*, 2824–2826.
- (30) Saraji, M.; Bakhshi, M. *J. Chromatogr., A* **2005**, *1098*, 30–36.
- (31) Swager, T. M. *Acc. Chem. Res.* **1998**, *31*, 201–207. Lee, D. W.; Swager, T. M. *Synlett* **2004**, 149–154.
- (32) Hass, K. C.; Schneider, W. F.; Curioni, A.; Andreoni, W. *Science* **1998**, *282*, 265–268. McHale, J. M.; Auroux, A.; Perrotta, A. J.; Navrotsky, A. *Science* **1997**, *277*, 788–791.
- (33) Kwon, D. H.; Kim, K. M.; Jang, J. H.; Jeon, J. M.; Lee, M. H.; Kim, G. H.; Li, X. S.; Park, G. S.; Lee, B.; Han, S.; Kim, M.; Hwang, C. S. *Nat. Nanotechnol.* **2010**, *5*, 148–153. Kim, S.; Choi, Y. K. *IEEE Trans. Electron Devices* **2009**, *56*, 3049–3054.
- (34) Panzer, M. J.; Frisbie, C. D. *J. Am. Chem. Soc.* **2007**, *129*, 6599–6607. Kaake, L. G.; Zou, Y.; Panzer, M. J.; Frisbie, C. D.; Zhu, X. Y. *J. Am. Chem. Soc.* **2007**, *129*, 7824–7830.
- (35) Santos, M. J. L.; Brolo, A. G.; Girotto, E. M. *Electrochim. Acta* **2007**, *52*, 6141–6145. Shoute, L.; Pekas, N.; Wu, Y.; McCreery, R. *Appl. Phys. A: Mater. Sci. Process.* **2011**, *102*, 841–850.